ROBOMECH Journal

RESEARCH Open Access

Agriculture aid for harvesting and pruning

Francesco Cepolina[1*], Gabriele Reverberi[1], Matteo Zoppi[1], Francesco Crenna[2], Mirko Job[3], Benedetto Giardulli[3] and Marco Testa[3]

Abstract

Farmers working on steep terrain need comfortable tools to improve their working conditions. Olive harvesting, which uses long unbalanced tools for reaching high branches, causes back pain. The posture of farmers, during harvesting operations, has been studied to determine the factors that are relevant in the evaluation of physical fatigue. The paper describes an exoskeleton designed to assist farmers during harvest and pruning. The exoskeleton, worn by the farmer, offers an additional arm to support the harvester. The proposed exoskeleton uses a spring to better balance the weight of the tool on the user's body, reducing the weight on the upper limbs. The kinematics of the selected architecture is analysed. The exoskeleton is discussed with an emphasis on its advantages and disadvantages. A group of operators has tested the exoskeleton on the field. Myoelectric tests have been performed to evaluate the fatigue. The results are positive, the exoskeleton reduces the perceived load, allowing sufficient dexterity to work outdoors. The research shows that it is possible to create inexpensive exoskeletons for agriculture. The proposed exoskeleton can also be successfully used for branching, painting, and cleaning glass.

Keywords Exoskeleton, Passive exoskeleton, Agriculture, Olive harvesting, Harvest, Prune

Introduction

When large machinery cannot be utilized on steep terrains, work is primarily done by hand with the aid of manual tools. For instance, the geomorphological structure of Liguria, a sea-facing region of northern Italy, is primarily characterized by hilly areas where most farming is done on terraces. Because of this, farming is much harder [1] and costlier than operating on flat terrain. The growth of a mechanized sector is hampered by this region's peculiarities, complexity, and small company sizes. In challenging areas like Ligurian terraces, commercial systems are restricted. Therefore, there is weak commercial demand. Standard-sized tractors cannot be driven easily along terraced strips: only small, tracked vehicles can be deployed [2]. Large corporations are not compelled to create "ad hoc" technology since there is little market demand, and those created for flat regions are sometimes useless or unaffordable for small regional businesses. In olive harvesting operations, the most popular method is the "beat down" also known as "fluttering" due to the movement imparted to the fronds to detach fruits from branches and collect them on nets placed underneath. This method was developed to speed up harvesting activities in the conventional harvesting system, which used bamboo canes as a tool. The harvesting methods are gradually becoming more sophisticated with the spreading of electric and pneumatic harvesters. Harvesters have inflexible rods that keep the oscillating comb in contact with the tree fronds. They occasionally have

*Correspondence:
Francesco Cepolina
francesco.cepolina@edu.unige.it
[1]Department of Mechanical, Energy, Management and Transport Engineering – DIME, University of Genoa, Genoa, Italy
[2]Measurement and Biomechanics Lab – DIME, University of Genoa, Genoa, Italy
[3]Department of Neuroscience, Rehabilitation, Ophthalmology, Genetics and Maternal and Child Sciences – DINOGMI, University of Genoa, Genoa, Italy

telescopic extensions that let the user reach branches that are 3–4 m above the ground. The first powered harvesters were machines with vibrating combs at the ends that were powered by compressed air. The systems that use pneumatic driving require a central unit to produce compressed air; this device is often a mobile commercial compressor that is coupled to a power supply generator. From the compressor to the harvester, there must be several meters of tubing for air distribution. The benefits of reduced weight have gradually been eclipsed by electrically powered devices' great performance (Fig. 1). A passive exoskeleton actuated by linear springs and specifically tailored for agricultural tasks is described in this paper.

State of art

Today, it is possible to wear an exoskeleton that increases the power of the user, fulfilling ancient longing. Active exoskeletons and smart wearables are devices too sophisticated and delicate to be used in humid and dusty agricultural environments. Many active exoskeletons are motor-driven, making them heavy, increasing user metabolic cost, and limited by battery life, which is impractical for prolonged field use [3, 4]. Soft exoskeletons reduce fatigue of the upper limbs [3, 4]. The optimization of the backpack suspension may lead to obtaining better energy efficiency [5]. The use of backlash for the connection elements also improves the exoskeleton's performance [6]. Supernumerary robotic limbs may help to handle more tools at the same time [7]. Several examples of active military exoskeletons already exist in the rehabilitation [8–11] and military field. Current passive exoskeleton technologies offer various forms of assistance across different body parts and tasks. A selection of commercial passive exoskeletons is now recalled. These devices are subdivided in two categories: back support and upper limb support.

The EXOVITI exoskeleton is a passive device using two springs to support the back during forward-bending tasks common in agriculture, such as pruning and hoeing. It reduces the load on lumbar back muscles and limits spine disk compression, while keeping the back aligned and reducing fatigue. Laevo is a passive back-support exoskeleton, using flexible elements to store energy. It is tested in material handling and order-picking tasks. Rakunie is a passive exoskeleton using elastic slings for entire body support, also perceived positively in order picking activities. IPAE is a passive back-support exoskeleton that includes ropes from the shoulder structure to the hands, designed to bypass the arms for load carrying. The Hero Wear Apex uses two long elastic elements positioned at the back of the operator to reduce back muscle activity.

The CDYS is a passive shoulder support exoskeleton for tasks requiring continuous or repetitive arm lifting. A spring system is linked to the belt around the waist: two cables connect the springs to the shoulders. Its design transfers the weight to a waist belt to avoid spinal loading. The HAPO line includes lightweight models like the HAPO FRONT (1.3 kg) and HAPO UP (1.67 kg). The HAPO UP assists with overhead arm movements (60°-180° vertically) for light loads, while the HAPO FRONT targets "arms forward" postures (0°-135° vertically). The Levitate Airframe is a passive upper-limb exoskeleton, showing improved time and quality during simulated static holding tasks and a deltoids and trapezius muscle

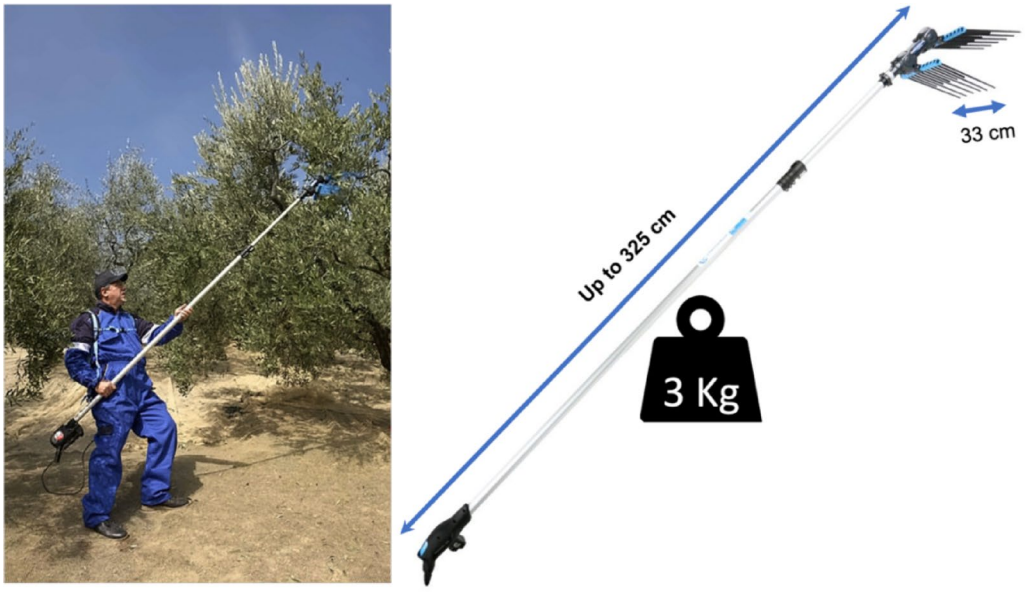

Fig. 1 Long olive harvester powered by an electric motor. Courtesy of Campagnola company

activity reduction in real overhead assembly tasks in the automotive industry. Paexo shoulder is a passive upper-limb exoskeleton reduces deltoids activity, and increased biceps activity.

Design and characterization

Existing exoskeleton solutions do not directly provide the dedicated tool support required for effectively handling long, unbalanced agricultural implements. While passive, many current exoskeletons are still too delicate for harsh agricultural environments, which are frequently humid, dusty, and prone to shocks, requiring robust mechanical elements. User discomfort at contact points, where the device interfaces with the body, is a commonly reported disadvantage across various exoskeletons. Some designs, particularly those with rigid structures or for tool support, can cause movement interference and reduce dexterity or range of motion for the user.

This paper introduces a novel exoskeleton specifically designed to address the unique ergonomic challenges faced by farmers working on steep terrains, especially in olive harvesting. The proposed exoskeleton has been designed, prototyped, built, and tested to enable olive harvesting on steep terrain or in circumstances that do not lend themselves to the use of heavy machinery [12–14]. Unlike general support exoskeletons, this device is engineered as an additional limb to directly support long, unbalanced agricultural tools like olive harvesters. This specific functional design reduces the weight and torque strain on the user's upper limbs and back, providing a distinct kinematic approach to directly mitigate fatigue from handling these implements.

It employs a passive architecture, relying on robust mechanical elements such as rotating joints and steel springs for load compensation. The proposed exoskeleton is inexpensive, simple to maintain and repair, and durable enough to withstand the demanding, often humid, dusty, and shock-prone agricultural environments, unlike more delicate active or complex passive systems. Its design focuses on redistributing forces and torques to a semi-rigid structure on the lower back, with optional additional support from the upper back and shoulders. This strategy specifically avoids direct spinal loading and preserves the user's overall mobility.

This affordable device is intended to assist farmers who handle uneven loads regularly (Fig. 2). The relative position of the waist of the farmer and the pole of the harvesting tool can be perpendicular or parallel. A virtual 3D mock-up was created to better show these two positions.

The farmer needs both hands to sustain the long tool without the aid of an exoskeleton (Fig. 2a). A high torque is generated to balance the tool [15–17]. Owing to the size of the harvesting tool, the farmer cannot place it all in front of his body but needs to place it aside (Fig. 2c). To better counterbalance the long and heavy tools, the farmer places them close to his body (Fig. 2c). When feasible, the farmer tends to keep the feet still and rotate the tool, to reach the branches of the tree close to them. Rotations of the torso are typically performed to better reach the desired positions. For better balance, the hands are placed far each other (Fig. 2a-d). All the muscles of the upper torso and arms must cooperate to lead and use this tool (Fig. 2e). Some models of olive harvesters are motorized, which creates additional stress on the farmer's body. The farmer needs to constantly look up at the branches (Fig. 2f) searching for olives. This position at the end of the day causes neck aches. The repetitive movement of farmers carrying heavy unbalanced loads

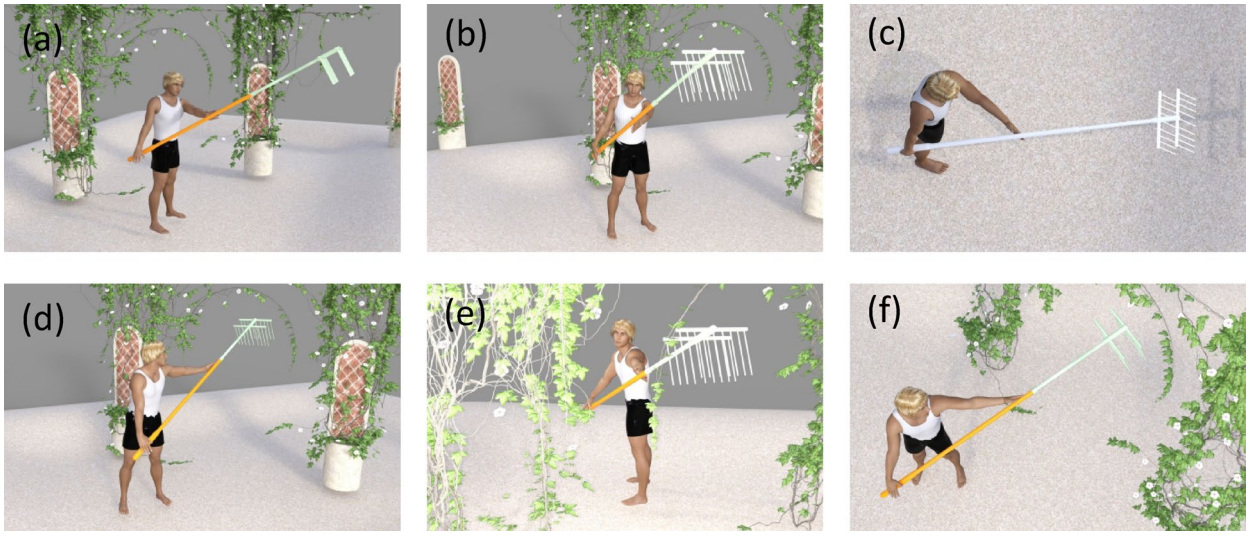

Fig. 2 3D representation of harvester working positions. Waist and tool-perpendicular views: side (**a**), front (**b**), and top (**c**). Waist and tool parallel views: side (**d**), front (**e**), and top (**f**)

represents a risk for musculoskeletal disorders [18–20]. The cinematic system of the proposed exoskeleton has been also examined.

Engineering constraints

When it comes to wearable robotics, human and robot interaction is intense [21], and the ergonomics of the exoskeleton are a key consideration [22]. Standardizing farmers' motions during the harvesting process is a vital initial step. Delicate mechanical or electronic components can easily be damaged by dampness, dust, or shock. These elements must be avoided when considering the environment in which the exoskeletons are used.

The simplicity of maintenance and repair is another reason to avoid the use of electronics. In the implementation of the kinematic chains, the use of translational joints is minimized to the greatest extent possible because they are more susceptible to damage from shocks, oxidation, and dust than rotational joints. Additionally, the use of air or fluid springs is restricted for the reasons outlined above. Based on these assertions, the fundamental concept is to use rotating joints and steel springs for load compensation and torque counterbalancing [23–25].

Body interface constraints

Any solution that demands the implementation or compensation of loads on the lower limbs is rejected to retain the mobility of the operator as much as possible. Similarly, methods that boost performance using rigid connections, which conform to the anatomic profile of the elbow and wrist, are rejected to ensure proper mobility of the upper limbs. This limits the field to the employment of an external arm that must be attached to the operator's torso and kinematically separated from the two higher limbs [26, 27]. It is necessary to redistribute the forces and torques produced by the harvester by utilizing a stiff or semi-rigid interface with the body to preserve mobility and advance ergonomics. Currently, only six body parts — abdomen, hips, upper back, chest, lower back, and shoulders — can serve as potential interface locations (Fig. 3).

The analysis is performed by considering both physiological factors (such as skin average thickness, proximity to potential load-bearing structures, nociceptive nerve endings distribution), dynamical factors (load distribution on the musculoskeletal structures) and aspects connected to the range of motion required.

The option of using a rigid or semi-rigid plate on the abdomen to compensate for the pressures and torques involved is instantly rejected because it lacks a rigid bone structure [28]. Moreover, placing a solid structure in front of the abdomen would significantly reduce torso motion, especially abdominal flexion. In the event of a user's fall, interfacing the exoskeleton to the chest could lead to an equally high probability of head-tool collision and an overload of the lumbar vertebrae because the entire burden would need to be supported by the spine. Low spinal cord overload cannot be alleviated if only the upper back is used as the interface location. The same holds for shoulders that are the only interface [29–31]; however, when one shoulder is more solicited than the other, asymmetrical stress results. The only feasible position to interface is a semi-rigid structure on the lower back, which could also include additional support

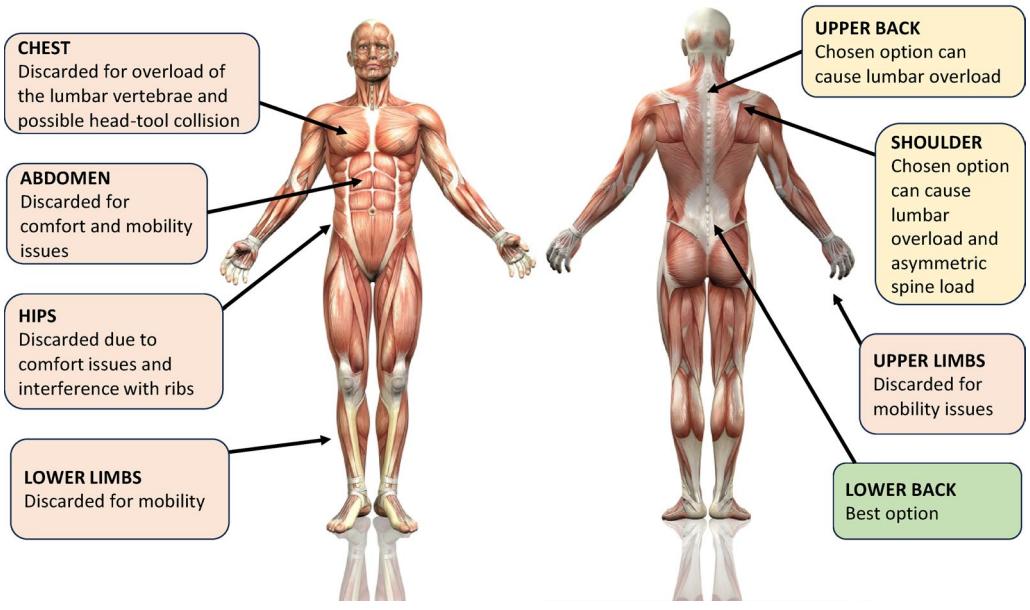

Fig. 3 Possible connection regions between the body and the exoskeleton (Image by kjpargeter on Freepik)

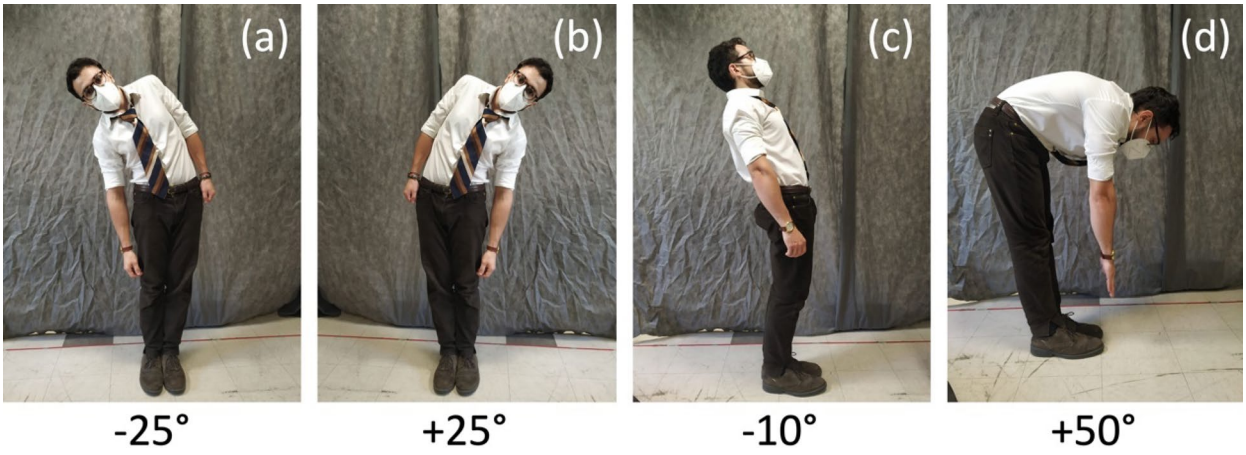

Fig. 4 Human torso mobility

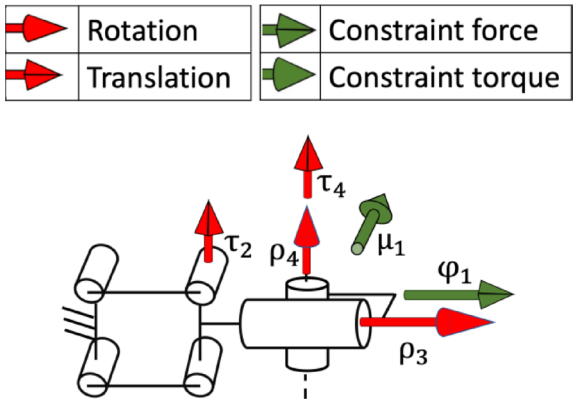

Fig. 5 Passive exoskeleton, kinematic chain

from the upper back and shoulders [32, 33] to prevent all the problems described above, as shown in Fig. 3. Wavy ribs may be compressed and subjected to impact when the plate is connected to the hips. The lumbar vertebrae may become overloaded if a rigid plate is solely attached to the upper back, chest, or shoulders, as the entire load must be supported by the spine. The lower back is the only position that can successfully establish a semirigid interface to meet these criteria.

In addition, placing a hard structure in front of the abdomen significantly reduces torso motion, which is at its greatest during abdominal flexion (Fig. 4). The kinematic and physical prototypes of the three exoskeletons of the family have now been revealed. Both the benefits and disadvantages are discussed.

Kinematic analysis

The exoskeleton adopts a compact architecture. A four-bar linkage, loaded with springs, compensates for the weight of the olive's harvester (Fig. 5).

The kinematic chain of the tool is now studied. To perform the constraint analysis, screw theory is used. For a chosen Cartesian frame in space, we associate a standard basis in the six-dimensional space of twists and the dual basis spans the dual space of wrenches. For rigid body L:

$$\mathrm{L} = 1 \tag{1}$$

The twist systems TL and PL are spanned by all joint screws and by the passive (non-actuated) screws. The reciprocal wrench systems are:

$$\mathrm{WL} = \mathrm{T} \perp \mathrm{L} \tag{2}$$

$$\mathrm{VL} = \mathrm{P} \perp \mathrm{L} \tag{3}$$

The entities of WL represent the leg structural constraints (also called as geometric or non-actuated constraints). These are the wrenches reciprocal to all the joint screws that the leg L can transmit when all its joints are left free to move. The space VL denotes the wrenches that component L can transmit when its actuated joint is locked. The wrenches in VL, reciprocal to the passive joint screws are called actuated constraints. M represents the twist system of the end-effector mobility in non-singular configuration. For any configuration we have:

$$\mathrm{TL} \supset \mathrm{PL} \tag{4}$$

$$\mathrm{WL} \subset \mathrm{VL} \tag{5}$$

In some singular postures, VL is also reciprocal to the screw of the actuated joint, then

$$\mathrm{TL} = \mathrm{PL} \tag{6}$$

$$\mathrm{WL} = \mathrm{VL} \tag{7}$$

Table 1 shows the constraint of each kinematic chain.

The user wears the exoskeleton. A four-bar linkage is linked to the back of the operator. The four-bar linkage

Table 1 Motion constraint reciprocity rule

Motion	Constraint	Reciprocity rule
Rotation	Force	Coplanar axes
Translation	Couple	Always
Rotation	Couple	Perpendicular
Translation	Force	Perpendicular

enables vertical span τ2. The cylindrical joint 3, linked to the free extremity of the four-bar linkage, and perpendicular to τ2, allows rotation ρ3. The cylindrical joint 4, is linked to joint 3. The axes of joints 3 and 4 are perpendicular. The cylindrical joint 4 enables vertical translation τ4 and rotation ρ4.

The kinematic chain structural constraint is the wrench ϕ1 (force), coplanar with ρ3 and ρ4, orthogonal with τ2 and τ4, and the wrench μ1 (couple) perpendicular to ρ3 and ρ4.

The articulated parallelogram, positioned on the back, and loaded with a spring, allows the harvester to be lifted and lowered effortlessly. The spring balances the weight of the harvester. Considering the configuration of the arm, its constraint analysis is:

$$dim\ T_1 = 4 \tag{8}$$

$$dim\ W_1 = 2 \tag{9}$$

$$Span\ T_1 = \tau_2, \rho_3, \rho_4, \tau_4 \tag{10}$$

$$Span\ W_1 = \varphi_1, \mu_1 \tag{11}$$

The following symbols have been adopted:

T_1, W_1: Vector spaces describing torques/forces and constraints.

τ_2, ρ_3, ρ_4, τ_4: Kinematic components along respective joint coordinates.

ϕ_1, μ_1: Dynamic constraints.

The torque space (T_1) has four dimensions, indicating 4 degrees of freedom or generalized coordinates influencing the system. The constraint wrench space (W_1) has two dimensions, meaning only two independent constraint directions (wrenches) are acting on the system.

Equations 8–11 define the mechanical constraints and actuation space of the exoskeleton's kinematic chain. They establish how many inputs/forces can act on the system (T_1), how many constraints restrict its motion (W_1), and what are the independent directions of those forces and constraints. This mathematical structure is used to model and analyze the static equilibrium of the exoskeleton under external loads.

The equations show that the exoskeleton system has 4 generalized actions and 2 constraints, leaving 2 degrees of freedom. This means it is not over constrained nor unstable, but intentionally underactuated to allow flexibility. These 2 DOFs correspond to key user motions (like lifting and orienting the tool). The design balances support and freedom, aiding movement without excessive stiffness. This guides smart placement of springs and joints for ergonomic efficiency.

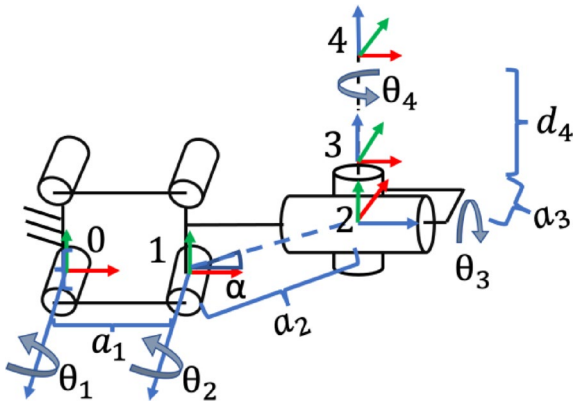

Fig. 6 Passive exoskeleton, Denavit-Hartenberg convention

Table 2 Denavit-Hartenberg parametrization

TYPE	Joint 1	Joint 2	Joint 3	Joint 4
	Revolute	Revolute	Revolute	Cylindrical
θ	0	α	θ_3	θ_4
d	0	0	0	d_4
a	a_1	a_2	a_3	0

Now, to fully assess the dynamics of the mechanism, the partial differentiation method is used.

First step is to establish a parametrization of the reference frames of each joint. For this aim Denavit-Hartenberg convention is used:

Each Z axis corresponds with the main axis of the joint: the rotation axis of the revolute joint, the translation axis of the prismatic joint

Each X axis can be arbitrarily assigned, but it's convenient to align it with the next joint.

Each Y must be chosen following the left-hand-rule.

Considering now each joint from 1 to n to have an assigned reference frame with origin On, the transformations of each joint with respect to its previous one can be described with the Denavit-Hartenberg parameters (Fig. 6).

dn: distance of On with respect to On – 1 on the Zn – 1 axis.

an: distance between Zn and Zn – 1 axis.

θn: rotation angle around Zn – 1 axis.

The mechanism is parametrized according the Denavit-Hartenberg convention The following parametrization can be obtained (Table 2). The parameters θ1 and θ2 are deliberately set to zero for the presence of the four-bar linkage. This choice has been adopted to simplify the kinematic evaluation and for the sake of brevity.

To describe a change of coordinates of the *n* reference frame with respect to the *n*-1, both the translational and the rotational components of motion must be kept into account, visually extrapolating from the geometry of the kinematic chain the displacement vectors $d_n^{n-1}$and the rotation matrices R_n^{n-1}. Using these two elements, it is possible to obtain the Transformation matrices T_n^{n-1} of a reference frame with respect to the previous one:

$$T_n^{n-1} = \begin{pmatrix} & R_n^{n-1} & & d_n^{n-1} \\ & & & \\ 0 & 0 & 0 & 1 \end{pmatrix} \tag{12}$$

Obtaining the transformation matrix T_i^{i-1} of an *i* reference frame with respect to the base-frame can be done by pre-multiplying it for the transformation matrices of all the previous reference frames:

$$T_i^0 = T_1^0 * T_2^1 * \ldots * T_i^{i-1} * \ldots * T_n^{n-1} \tag{13}$$

The component of the transformation matrices with respect to the base-frame will therefore be the rotation matrices and the displacement vectors with respect to the base-frame

$$T_n^0 = \begin{pmatrix} & R_n^0 & & d_n^0 \\ & & & \\ 0 & 0 & 0 & 1 \end{pmatrix} \tag{14}$$

The Jacobian matrix can therefore be computed for prismatic and revolute joints, by following Table 3:

Once the Jacobian matrix is computed, it is possible to transpose it and its product by the wrench ζ_e acting on the end effector, will give as a result the vector Φ, which components are the forces and torques to be applied at every joint to maintain the kinematic chain in equilibrium.

$$\Phi = J'\zeta_e \tag{15}$$

The gravitational component on the end-effector ζ_e is represented as:

$$\zeta_e = \begin{pmatrix} 0 \\ -\mathrm{mg} \\ 0 \\ 0 \\ 0 \\ 0 \end{pmatrix} \tag{16}$$

Transposing the Jacobian Matrix and multiplying it by the vector ζ_e (Principle of Virtual Work), we obtain the forces and torques of the joints to maintain the static balancing of the architecture.

$$\phi = \begin{pmatrix} -mg\left(a_1 + a_2\cos\alpha + \sigma_2 - \sigma_1\right) \\ -mg\left(a_2\cos\alpha + \sigma_2 - \sigma_1\right) \\ -mg\cos\alpha\left(d_4\cos\theta_3 + a_3\sin\theta_3\right) \\ -mg\cos\alpha\cos\theta_3 \end{pmatrix} \tag{17}$$

Where:

$$\sigma_1 = d_4 \sin\alpha \sin\theta_3 \tag{18}$$

$$\sigma_2 = a_4 \sin\alpha \cos\theta_3 \tag{19}$$

The following symbols are adopted in the Eq. 10 to 12:

a_1, a_2, a_3, a_4: link lengths or distances between joints.

d_4: displacement along joint 4.

α: fixed inclination angle (e.g., body or spring angle).

θ_3: joint angle at joint 3.

m: mass of the harvester/tool.

g: gravitational acceleration.

σ_1, σ_2: offset terms from joint displacement due to spring/linkage configuration.

Table 3 Linear and rotational joints

	prismatic	revolute	cylindrical
linear	$R_{i-1}^0 \begin{pmatrix} 0 \\ 0 \\ 1 \end{pmatrix}$	$R_{i-1}^0 \begin{pmatrix} 0 \\ 0 \\ 1 \end{pmatrix} X(d_n^0 - d_{i-1}^0)$	$R_{i-1}^0 \begin{pmatrix} 0 \\ 0 \\ 1 \end{pmatrix} + R_{i-1}^0 \begin{pmatrix} 0 \\ 0 \\ 1 \end{pmatrix} X(d_n^0 - d_{i-1}^0)$
rotational	$\begin{pmatrix} 0 \\ 0 \\ 0 \end{pmatrix}$	$R_{i-1}^0 \begin{pmatrix} 0 \\ 0 \\ 1 \end{pmatrix}$	$R_{i-1}^0 \begin{pmatrix} 0 \\ 0 \\ 1 \end{pmatrix}$

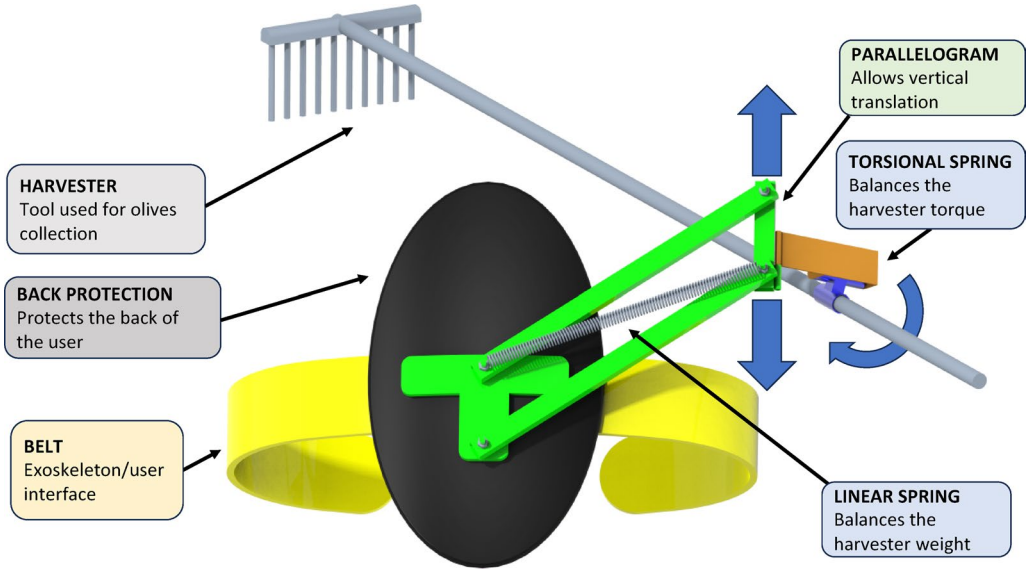

Fig. 7 Working principle of the exoskeleton

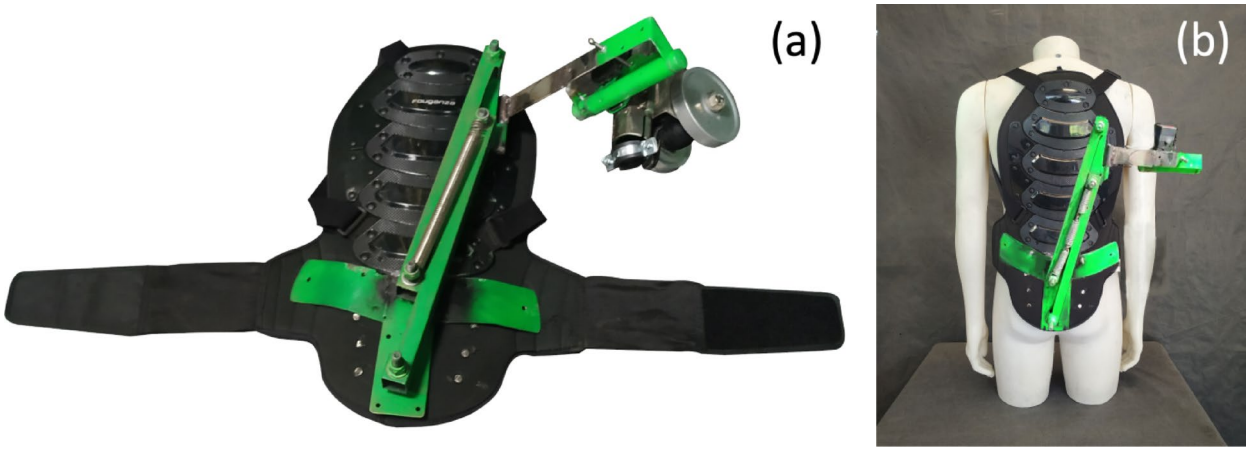

Fig. 8 Passive exoskeleton prototypes. Views: open (**a**), on a mannequin (**b**)

The vector ϕ of Eq. 5 represents the generalized force components (e.g., torques/forces) required at each joint to counterbalance the gravitational torque/force from the tool weight. Equation 10 represents the gravitational force vector acting on the harvester/exoskeleton system due to the tool's weight. It includes torques and forces needed at each joint to maintain static balance.

Equations 17 and 18 define geometrical offsets (σ_1, σ_2) used in calculating the vertical force/torque based on joint angles and link position. Together, they describe how load is distributed across the system depending on posture. These are used to compute how much mechanical support (torques/forces) the exoskeleton must generate at each joint to maintain static equilibrium while supporting the tool.

In addition, a spring winch system is added to withstand the axial force, caused by the weight of the harvester in a nearly vertical position. The main components of the proposed exoskeleton are shown in Fig. 7.

Prototype design

The prototype was built by connecting to the torso's rigid steel, "Y" shaped steel plate, held in position by a back protector with Velcro abdomen fastening and shoulder straps (Fig. 8 and b).

On this plate, two steel threaded pins are welded with an offset between their axes of approximately 10 cm in a position orthogonal to the human spine. These two pins are part of a steel four-bar linkage, with one shorter element corresponding with the back plate, the other one being approximately 12 cm in length and the two longer of approximately 35 cm. A spring can freely slide inside the longer parts' hollow "C" shape. In the second stage, an additional external spring for dampening was added.

A hinge is welded to the 4-bar linkage's end. A pre-loaded hinge is welded in an orthogonal direction to the axis of the preceding one on the lower knuckle of the third hinge. This mechanism's spring is loaded to withstand the momentum that the harvester causes. The parallelogram on the prototype's back is painted green, as shown in the photos (Fig. 8a-b).

Finally, to sustain the harvester and give it the possibility to slide, a release system is connected to the pre-loaded hinge via a car safety belt buckle, to quickly release the slider mechanism connected to the harvester. This system is obtained using two half-pipe sections, connected by two hinges from one side and having on the other side two lever buckles as a fastening system (a shell-like mechanism). When not loaded the four-bar linkage practically disappears (Fig. 8b).

Field prototype evaluation

The exoskeleton proposed is now evaluated by 15 individuals specialised in oliviculture. The individuals, ranging from 18 to 70 years, have the following characteristics: Mean (average) age: 43.1, Median age: 47, Mode (most frequent age): 23, Standard deviation: ≈ 15.4. The sample consist of 86.7% male and 13.3% female.

The exoskeleton has the task of evenly loading the body. Various factors have been evaluated. The best exoskeleton is light (light), low price (cheap), easy to handle (dexterous) and pleasant to wear (comfort). It allows one to reach a wide work area (agile). It requires low maintenance (rugged). The farmers wish to wear the exoskeleton without help (wearable). The link between the harvester and the exoskeleton must be natural (intuitive). The average mark of all the evaluation parameters is also calculated (total score). The results of the on-field tests are reported (Fig. 9).

The dexterity of the exoskeleton is good: the operator can easily harvest a relatively large surface without moving.

According to the needs the tip of the harvester can be positioned low or high (Fig. 10). The close view allows to see details of the tool in action.

The harvester can be easily removed, and the exoskeleton is light (fast-lock mechanism). When the tool is close to vertical, keeping the cylindrical joint at the end of the arm, does not ensure proper operation of the four-bar linkage. This lightweight exoskeleton is comfortable and easy to wear. The prototype's limitations are related to ease of use: farmers feel that the exoskeleton does not allow to make intuitive movements (intuitive).

Evaluation of myoelectric manifestation of fatigue

Myoelectric tests conducted on the prototype have demonstrated a reduction in muscular fatigue, confirming its effectiveness in improving working conditions. The exoskeleton allows to support heavy, unbalanced tools using a single arm, allowing the farmer to keep a hand free for balance or other tasks, thus enhancing safety during operations on uneven terrain.

Some exoskeleton fatigue tests have been performed in the lab. Surface electromyography (sEMG) can provide useful information related to muscular fatigue. More specifically it has been shown that during an isometric fatiguing contraction, there is a general increase in the integrated electrical activity of the muscles with a shift in the power spectrum of the sEMG signals toward lower frequencies [34]. Hence, a preliminary evaluation was conducted using sEMG analysis to investigate the impact of the use of the proposed exoskeleton on muscular fatigue during simulated pruning activity in the laboratory.

The participant was a 30-year-old young healthy male (having a Body Mass Index BMI = 12%) with no comorbidities and/or history of musculoskeletal diseases. sEMG signals were acquired using six pairs of Ag/AgCl disposable adhesive circular surface electrodes (CDE02401500BX – SPES medica s.r.l.) 24 mm in diameter and 15 cm cable, positioned with an inter-electrode distance of 25 mm along the direction of the muscle

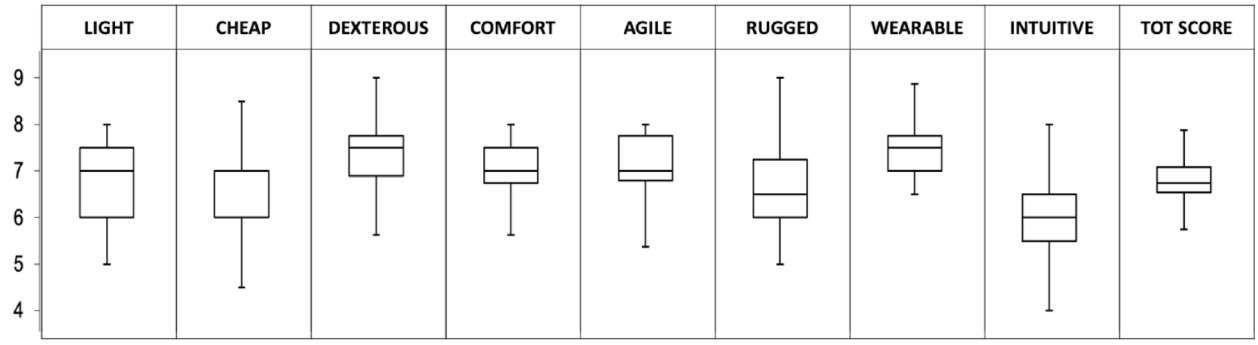

Fig. 9 Evaluation of the proposed exoskeleton by the 15 individuals. Each of the 15 individuals has given a score ranging from 0 to 10 (0 lowest score, 10 highest score)

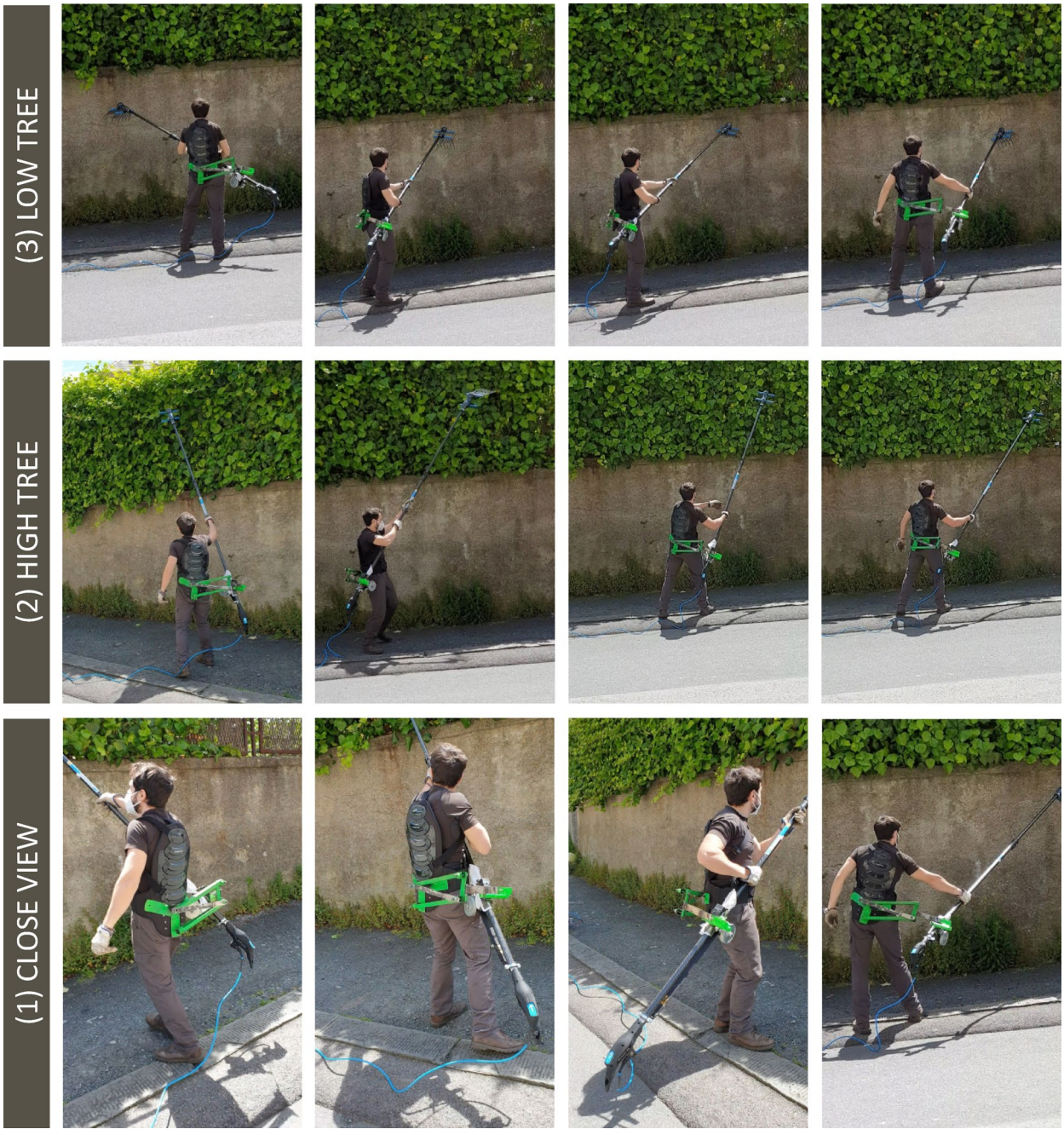

Fig. 10 Prototype in action

Table 4 Characteristics of the EMG amplifier

Differential Gain	**1000**
Input Impendence	> 90 MW
CMRR (Common Mode Rejection Ratio)	> 96 db
Equivalent Input Noise	< 0.8 µVrms (differential)
Nominal Band Pass Filter	10 : 750 Hz, Bessel
Sample Frequency	2048
Input Dynamic of the A/D Converter	0 : 5 V
A/D Resolution	12

fibres. Electrodes were placed following the SENIAM (Surface Electromyography for Non-Invasive Assessment of Muscles) guidelines for electrode placement [35] on the erector spinae (bilaterally), and on the left upper limb that held the harvester during the experimental task. More specifically, electrodes were positioned on the biceps brachi, on the lateral head of the triceps brachi, on the medial deltoid, and the superior trapezius. The reference electrode was placed on the left wrist. sEMG signals were acquired through the EMG-USB amplifier

(OTBioelettronica) in single differential mode with a gain of 1000 and a sampling frequency of 2048 Hz (Table 4).

The skin around the area of application of the electrodes was shaved and cleaned using a specific abrasive and conductive gel (EVERI – Spes medica S.r.l). The experimental protocol consisted of two primary phases: (i) a *fatiguing phase* during which the participant was instructed to repeat a series of pruning movements with the harvester toward six sequential targets on the laboratory (Fig. 11) wall until exhaustion; followed by a five-minute break, and (ii) an *evaluation phase* where the participant's sEMG activity was recorded while holding the harvester extended in front of them for as long as possible. The above protocol was repeated without (Natural - N) and with the aid of the proposed exoskeleton (Exoskeleton - E) with an 11-minute break separating the two experimental conditions. The sEMG signals were processed in MATLAB (MATLAB, The MathWorks Inc.) to extract information related to their amplitude and their frequency components. The total duration of the evaluation phase in both conditions was registered as a performance index of the experimental task.

Signals were detrended by removing their mean value and bandpass filtered between 20 Hz and 400 Hz using a 6th-order Butterworth filter. To obtain the amplitude of the muscle activity, the signals were full-wave rectified and the envelope of the sEMG was obtained through a 6th-order Butterworth low-pass filter at 10 Hz. A Time-Frequency analysis of the signal was carried out using the Short-Time Fourier Transform to calculate the median frequency of the power across windows of 500 ms with an overlap of 0.250 ms [36]. Descriptive statistics, including the median, first quartile, and third quartile of amplitude and frequency variables were computed independently for both experimental conditions. These statistics were calculated considering a time window corresponding to the shortest total duration achieved between the two conditions. This approach ensured uniformity in the number of data samples for the main outcomes, which were subsequently grouped into the beginning, middle, and final segments of the specified time window (BEG-MID-END).

Results are reported in Table 5 and displayed as boxplots in Figs. 12 and 13.

The findings are aligned with the literature, indicating an increase in the amplitude variables of the sEMG signal and a transition to lower frequencies in its power spectrum under fatigue. In natural conditions, the sEMG amplitude was consistently higher across all muscles compared to the exoskeleton condition. Additionally, a notable trend in the difference between the median frequencies of the power spectrum was observed for the biceps brachii, triceps brachii, deltoid, and erector spinae, in favour of the exoskeleton condition. The results

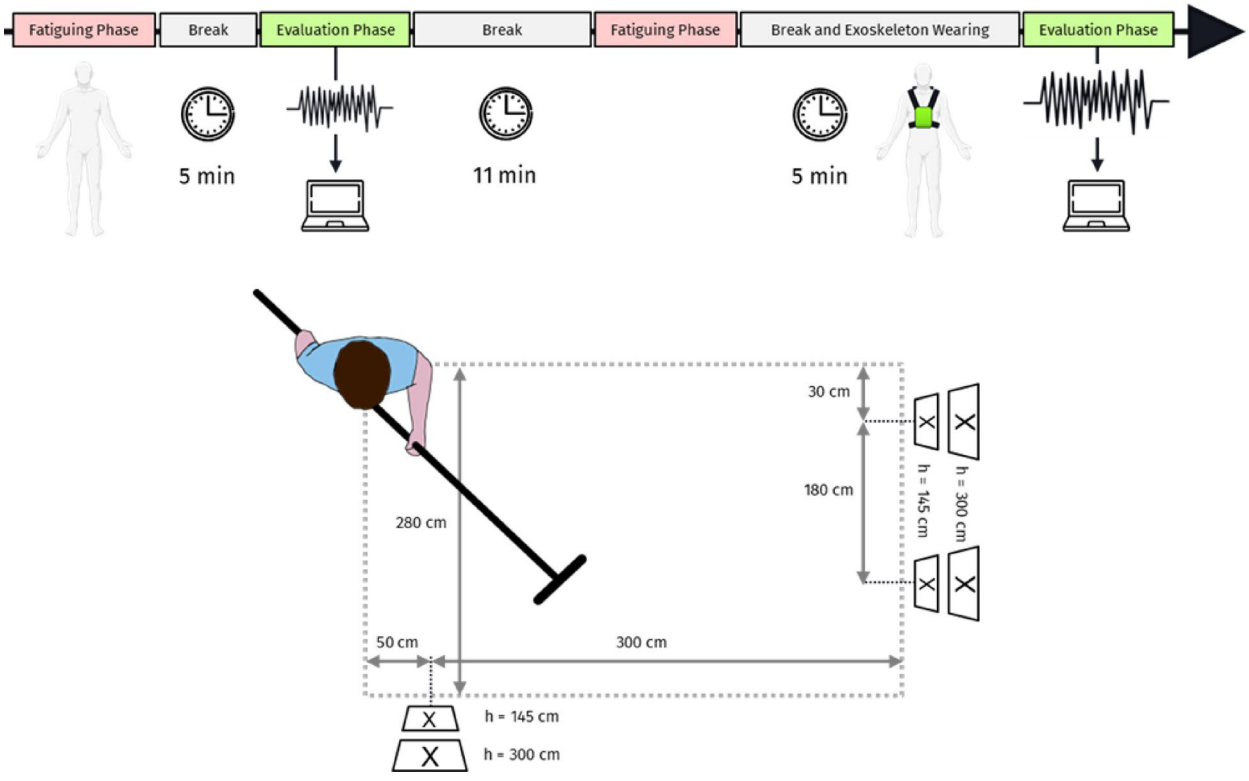

Fig. 11 Experimental Protocol and Experimental Setting

Table 5 Descriptive analysis of the variables obtained from the electromyographic analysis for both experimental conditions

Experimental Condition	***N***			**E**		
Total Time [min: sec]	**2:24**			**5:46 (interrupted by assessor for time limit)**		
	BEG	**MID**	**END**	**BEG**	**MID**	**END**
sEMG Amplitude [mV]						
Biceps Brachii	0.116	0.144	0.115	0.040	0.022	0.020
Triceps Brachii	0.026	0.024	0.026	0.004	0.012	0.015
Deltoid	0.028	0.021	0.023	0.006	0.007	0.006
Trapezius	0.123	0.151	0.117	0.048	0.012	0.015
Erector Spinae Left	0.025	0.025	0.031	0.018	0.017	0.017
Erector Spinae Right	0.035	0.037	0.035	0.020	0.021	0.020
Median Frequency [Hz]						
Biceps Brachii	52.273	44.647	45.634	64.733	64.599	97.553
Triceps Brachii	58.596	46.097	46.867	77.665	81.427	94.048
Deltoid	62.769	53.672	60.488	69.114	69.923	73.452
Trapezius	69.402	69.215	67.817	60.007	57.673	60.432
Erector Spinae Left	93.344	88.958	88.498	105.429	105.063	103.117
Erector Spinae Right	90.495	86.147	87.179	95.535	97.964	97.032

Values are reported as median (Q1, Q2) for beginning (BEG), middle (MID), and final segments (END). Two conditions are compared: "Natural" user using the tool without exoskeleton (N) and "Exoskeleton" user using the tool with the exoskeleton (E)

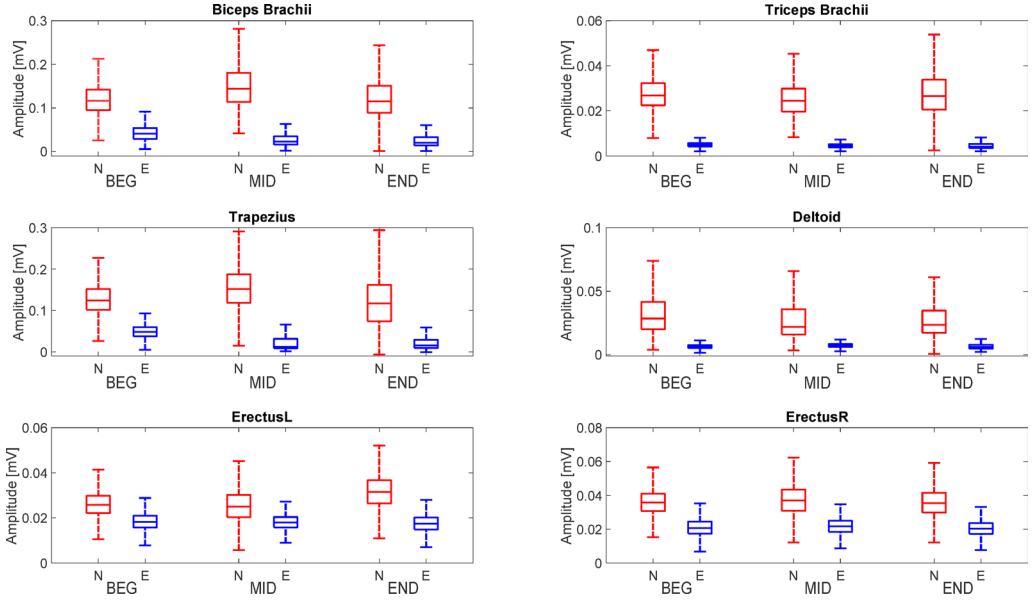

Fig. 12 Box plot of the data distribution related to the sEMG amplitude across the two conditions (N-natural, E-exoskeleton) and the three sequential phases of the time window for beginning (BEG), middle (MID), and final segments (END). The words ErectusL and ErectusR represents respectively: Left and right Erector Spinae (back muscle)

obtained show that the use of the exoskeleton reduced the effects of muscular fatigue. Under this particular condition, it is possible that the pool of recruitable motor units comprehended larger and less fatigue-resistant muscle fibres, characterised by a higher conduction velocity, which ultimately results in a lower electrical amplitude and higher frequency components of the sEMG signals [37].

Conclusion

An exoskeleton has been developed to assist Ligurian farmers during olive harvesting operations. Field tests have demonstrated that, in terms of movement amplitude (appropriate for harvesting operations), the proposed exoskeleton gives good and comparable performances. Specific myoelectric tests confirm that the proposed passive exoskeletons can be used effectively to reduce operator fatigue.

The exoskeleton is specifically designed to function as an "additional arm" to support long, unbalanced tools,

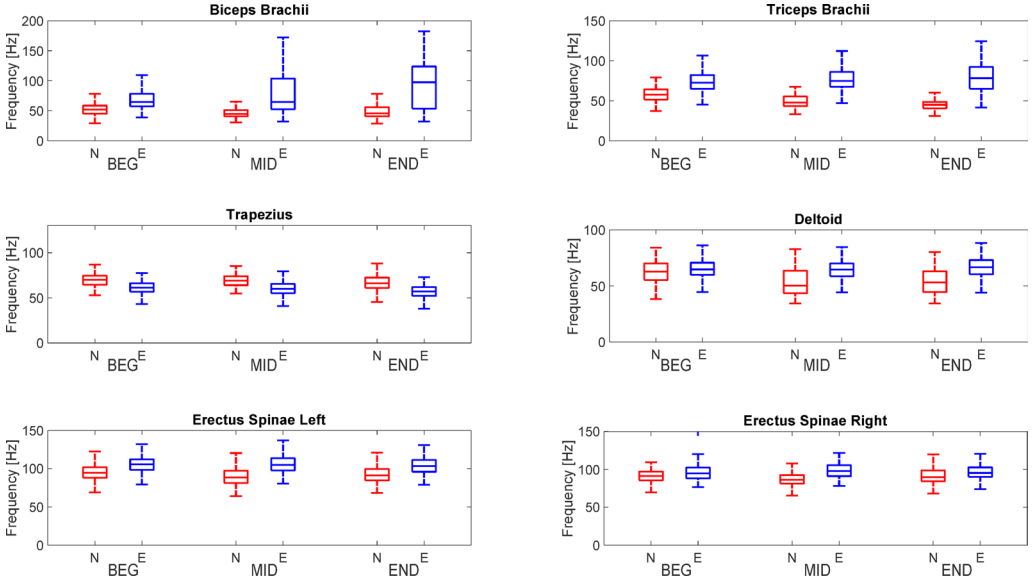

Fig. 13 Box plot of the data distribution related to the sEMG median frequency across the two conditions (N-natural, E-exoskeleton) and the three sequential phases of the time window for beginning (BEG), middle (MID), and final segments (END)

such as olive harvesters, directly reducing weight and torque strain on the user's upper limbs and back. This addresses a specialized need where conventional machinery is impractical, and manual labour poses substantial musculoskeletal risks. The design prioritizes a passive architecture that uses durable mechanical components, like rotating joints and steel springs, for load compensation. This ensures the exoskeleton is affordable, easy to maintain and repair, and robust enough to endure the humid, dusty, and shock-prone conditions of agricultural environments. Its emphasis on robust mechanical simplicity and cost-effectiveness addresses critical practical considerations for exoskeleton deployment. It is designed to redistribute forces and torques to a semi-rigid structure on the lower back, with optional additional support from the upper back and shoulders, to prevent direct spinal loading and maintain user mobility. The design specifically avoids rigid connections at the elbow and wrist to preserve upper limb dexterity.

Myoelectric tests performed on the prototypes have shown a reduction in muscular fatigue, confirming the effectiveness of passive exoskeletons in improving working conditions and aligning with the goal of reducing physical stress and strain.

Although generally described as lightweight, its primary construction from steel might imply it could be heavier compared to exoskeletons that extensively utilize carbon fiber, such as the CDYS or HAPO models. The use of a rigid steel plate for torso connection could, in some situations, contribute to thermal discomfort or interfere with movement. The cylindrical joint at the end of the arm does not operate correctly when the tool is positioned very close to vertical.

The arm reduces the work effort, while the back shield safeguards the spine from unintentional falls. The exoskeleton gives the farmer a second "safety feature" by enabling them to always have a free hand for balancing.

The exoskeleton was created expressly to address Liguria's harvesting issue (Italy). The Mediterranean region, where olive trees are grown, is the intended market for the "exoskeleton for the olive harvester." Exoskeletons can serve a variety of additional purposes, such as supporting long, rather heavy instruments in general. Cutting tree branches, applying copper fungicide, washing skyscraper windows, and roll-painting walls are just a few examples of the use cases.

Acknowledgements
The research was conducted in the framework of the S.IN.O.L. [Safety Innovation Oliviculture Liguria] project. The S.IN.O.L. project's principal partners are the CIPAT Centre for Professional Education and Technical Assistance of CIA, the CIA Italian Agricultural Confederation, the Cooperative of Sestri olive growers, and the University of Genoa. The project is fully funded by the Italian program "Measure 16.1 of the Rural Development Programme 2016–2020 of the Liguria Region IEP". The goal of the measure is in line with the European Innovation Partnership for Agricultural Productivity and Sustainability (EIP-AGRI) Focus Group.

Author contributions
All authors wrote the main manuscript text All authors wrote prepared the figures.F.C. and G.R. reviewed the manuscript.

Funding
Open access funding provided by University of Genoa within the CRUI-CARE Agreement. This project has received funding from the Italian program "Measure 16.1 of the Rural Development Programme 2016–2020 of the Liguria Region IEP".

Data availability
No datasets were generated or analysed during the current study.

Declarations

Ethics approval and consent to participate

This study obtained ethical approval from the Ethics Committee for University Research (CERA) of the University of Genova (approval date: 20/10/2022; CERA2022.47).

Competing interests

The authors declare no competing interests.

Received: 7 October 2024 / Accepted: 19 September 2025
Published online: 17 February 2026

References

1. Giardulli B, Battista S, Sansone LG, Leuzzi G, Giordano R, Testa M (2025) Exploring musculoskeletal pain among Italian Olive pickers: a cross-sectional investigation into prevalence, attitudes, expectations, and beliefs. Work 10519815241304999
2. Cepolina F, Reverberi G, Zoppi M, Pietronave G (2024) The forest Lift, a rugged tool to simplify pruning and fruit collection. Eng Agric Environ Food 17(1):37–45
3. Nassour J, Zhao G, Grimmer M (2021) Soft pneumatic elbow exoskeleton reduces the muscle activity, metabolic cost and fatigue during holding and carrying of loads. Sci Rep 11:12556
4. Firouzi V, Davoodi A, Bahrami F et al (2021) From a biological template model to gait assistance with an exosuit. Bioinspir Biomim 16:066024
5. Keren R, Or Y (2018) Energy performance analysis of a backpack suspension system with a timed clutch for human load carriage. Mech Mach Theory 120:250–264
6. Shafiei M, Behzadipour S (2020) Adding backlash to the connection elements can improve the performance of a robotic exoskeleton. Mech Mach Theory 152:103937
7. Tong Y, Liu J (2021) Review of research and development of supernumerary robotic limbs. IEEE CAA J Autom Sin 8:929–952
8. Zuo S, Li J, Dong M, Li G, Zhou Y (2021) Optimum design and preliminary experiments of a novel parallel end traction apparatus for upper-limb rehabilitation. Front Mech Eng 1–21
9. Shi D, Wang L, Zhang Y, Zhang W, Xiao H, Ding X (2022) Review of human—robot coordination control for rehabilitation based on motor function evaluation. Front Mech Eng 17(2):28
10. Proud JK, Lai DT, Mudie KL, Carstairs GL, Billing DC, Garofolini A, Begg RK (2022) Exoskeleton application to military manual handling tasks. Hum Factors 64(3):527–554. https://doi.org/10.1177/0018720820957467
11. Perez CN, Georgilas I, Etoundi AC, Chong J, Jafari A (2018) A conceptual exoskeleton shoulder design for the assistance of upper limb movement. In Towards Autonomous Robotic Systems: 19th Annual Conference, TAROS 2018, Bristol, UK July 25–27, Proceedings 19. Springer International Publishing, pp 291–302
12. Kong YK, Kim JH, Shim HH, Shim JW, Park SS, Choi KH (2023) Efficacy of passive upper-limb exoskeletons in reducing musculoskeletal load associated with overhead tasks. Appl Ergon 109:103965. https://doi.org/10.1016/j.apergo.2023.103965
13. Huysamen K, Bosch T, De Looze M, Stadler KS, Graf E, O'Sullivan LW (2018) Evaluation of a passive exoskeleton for static upper limb activities. Appl Ergon 70:148–155
14. Alemi MM, Geissinger J, Simon AA, Chang SE, Asbeck AT (2019) A passive exoskeleton reduces peak and mean EMG during symmetric and asymmetric lifting. J Electromyogr Kinesiol 47:25–34
15. Acosta AM, Benes JL, Haut BH, Gudukas TL, Laughlin JJ, Saltzman SM, Dewald JP (2003) A. Upper extremity multi-degree of freedom torque generating abilities in able-bodied individuals. 25th Annual International Conference of the IEEE EMBS, Cancun, Mexico, pp 1429–1432
16. Reverberi G, Cepolina F, Pietronave G, Testa M, Ramadoss V, Zoppi M (2023) The minimal exoskeleton, a passive exoskeleton to simplify pruning and fruit collection. Eng Agric Environ Food 16(1):37–42. https://doi.org/10.37221/eaef.16.1_37
17. Cepolina F, Crenna F, Reverberi G, Zoppi M (2024) Development of exoskeletons and motion measurement to reduce Olive harvesting labor. Eng Agric Environ Food 17(2):66–73
18. Davis KG, Kotowski SE (2007) Understanding the ergonomic risk for musculoskeletal disorders in the united States agricultural sector. Am J Ind Med 50(7):501–511
19. Tatar V, Yazicioglu O, Ayvaz B (2023) A novel risk assessment model for work-related musculoskeletal disorders in tea harvesting workers. J Intell Fuzzy Syst 1–19. https://doi.org/10.3233/JIFS-222652
20. Cecchini M, Bedini R, Mosetti D, Marino S, Stasi S (2018) Safety knowledge and changing behaviour in agricultural workers: an assessment model applied in central Italy. Saf Health Work 9(2):164–171
21. Molfino R, Cepolina FE, Cepolina E, Cepolina EM, Cepolina S (2023) Robots trends and megatrends: artificial intelligence and the society. Industrial Robot: Int J Rob Res Application. https://doi.org/10.1108/IR-05-2023-0095
22. Schiele A (2008) Fundamentals of ergonomic exoskeleton robots, 2008
23. Liang JJY, Zhang QH, Liu Y et al (2022) A review of the design of load-carrying exoskeletons. Sci China Tech Sci 65:2051–2067. https://doi.org/10.1007/s11431-022-2145-x
24. De la Tejera J, Bustamante-Bello R, Ramirez-Mendoza RA, Izquierdo-Reyes J (2020) A systematic review of exoskeletons towards a general categorization model proposal. Appl Sci 11(12):1–25
25. Pons JL (2008) Wearable robots: biomechatronic exoskeletons. Wiley
26. Gull MA, Bai S, Bak T (2020) A review on design of upper limb exoskeletons. Robotics 9(1):16. https://doi.org/10.3390/robotics9010016
27. Öçal AE, Lekesiz H, Çetin ST (2023) The development of an innovative occupational passive upper extremity exoskeleton and an investigation of its effects on muscles. Appl Sci 13(11):6763. https://doi.org/10.3390/app13116763
28. Mammone T, Metruccio F, Vida P, Moretto A (2007) The Italian system of data reporting in agriculture occupational health: a critical appraisal. J Public Health 15(4):301–313
29. Bitikofer CK, Hill PW, Wolbrecht ET, Perry JC (2018) Analysis of shoulder displacement during activities of daily living and implications on design of exoskeleton robotics for assessment. In Converging Clinical and Engineering Research on Neurorehabilitation III: Proceedings of the 4th International Conference on NeuroRehabilitation (ICNR October 16–20, 2018, Pisa, Italy 5. Springer International Publishing, pp. 478–482
30. Van der Have A, Van Rossom S, Rossini M, Jonkers I (2020) Effect of a new passive shoulder exoskeleton on the full body musculoskeletal load during overhead work. In Wearable Robotics: Challenges and Trends: Proceedings of the 5th International Symposium on Wearable Robotics, WeRob2020, and of WearRAcon Europe 2020, October 13–16, Springer International Publishing, pp. 165–169
31. Loh BG, Rosen J (2013) Kinematic analysis of 7 degrees of freedom upper-limb exoskeleton robot with Tilted shoulder abduction. Int J Precis Eng Manuf 14:69–76
32. Nasr A, Bell S, McPhee J (2023) Optimal design of active-passive shoulder exoskeletons: a computational modeling of human-robot interaction. Multibody SysDyn 57(1):73–106
33. Crea S, Cempini M, Moisè M, Baldoni A, Trigili E, Marconi D, Cortese M, Giovacchini F, Posteraro F, Vitiello N (2016) Validation of a gravity compensation algorithm for a shoulder-elbow exoskeleton for neurological rehabilitation. In Converging Clinical and Engineering Research on Neurorehabilitation II: Proceedings of the 3rd International Conference on NeuroRehabilitation (ICNR October 18–21, 2016, Segovia, Spain. Springer International Publishing, pp. 495–499
34. Naeije M, Zorn H (1982) Relation between EMG power spectrum shifts and muscle fibre action potential conduction velocity changes during local muscular fatigue in man. Eur J Appl Physiol Occup Physiol 50(1):23–33. https://doi.org/10.1007/BF00952241
35. Hermens HJ, Biomedical C (1999) of the E. C., & Programme, H. R. European Recommendations for Surface Electromyography: Results of the SENIAM Project. Roessingh Research and Development. https://books.google.it/books?id=w7HgOwAACAAJ
36. Dantas JL, Camata TV, Brunetto MAC, Moraes AC, Abrão T, Altimari LR (2010) Fourier and wavelet spectral analysis of EMG signals in isometric and dynamic maximal effort exercise. In: Annual International Conference of the IEEE Engineering in Medicine and Biology Society. IEEE Engineering in Medicine and Biology Society. Annual International Conference, 2010, pp 5979–5982. https://doi.org/10.1109/IEMBS.2010.5627579

37. Boccia G, Dardanello D, Tarperi C, Rosso V, Festa L, Torre AL, Pellegrini B, Schena F, Rainoldi A (2017) Decrease of muscle fiber conduction velocity correlates with strength loss after an endurance run. Physiol Meas 38(2):233. https://doi.org/10.1088/1361-6579/aa5139

Publisher's Note